Published in final edited form as:
Med Sci Sports Exerc. 2011 March ; 43(3): 525–532. doi:10.1249/MSS.0b013e3181f23fe8.

Hamstring Musculotendon Dynamics during Stance and Swing Phases of High Speed Running

Elizabeth S. Chumanov[1], **Bryan C. Heiderscheit**[1], and **Darryl G. Thelen**[1]
[1] University of Wisconsin-Madison, Madison, WI

Abstract

Introduction—Hamstring strain injuries are common in sports that involve high speed running. It remains uncertain whether the hamstrings are susceptible to injury during late swing phase, when the hamstrings are active and lengthening, or during stance, when contact loads are present. In this study we used forward dynamic simulations to compare hamstring musculotendon stretch, loading and work done during stance and swing phases of high speed running gait cycles.

Methods—Whole body kinematics, EMG activities and ground reactions were collected as 12 subjects ran on an instrumented treadmill at speeds ranging from 80% to maximum (average of 7.8 m/s). Subject-specific simulations were then created using a whole body musculoskeletal model that included fifty-two Hill-type musculotendon units acting about the hip and knee. A computed muscle control algorithm was used to determine muscle excitation patterns that drove the limb to track measured hip and knee sagittal plane kinematics, with measured ground reactions applied to the limb.

Results—The hamstrings lengthened under load from 50% to 90% of the gait cycle (swing), and then shortened under load from late swing through stance. While peak hamstring stretch was invariant with speed, lateral hamstring (biceps femoris) loading increased significantly with speed, and was greatest during swing at the fastest speed. The biarticular hamstrings performed negative work on the system only during swing phase, with the amount of negative work increasing significantly with speed.

Conclusion—We concluded that the large inertial loads during high speed running appear to make the hamstrings most susceptible to injury during swing phase when compared to stance phase. This information is relevant for scientifically establishing effective muscle injury prevention and rehabilitation programs.

Keywords

Acute strain injury; motion analysis; forward dynamic simulation; musculoskeletal model; muscle mechanics

Introduction

Muscle strains are a common injury among athletes, with the hamstrings being particularly susceptible to injury in sports that involve high speed running (16,28,41,52). For example, musculotendon strains accounted for nearly half of all injuries for a National Football League team during pre-season practice, with hamstring strains being the most common and requiring the most time (average of 8.3 days) away from sport (14). Similarly in the

Address correspondence to: Elizabeth S. Chumanov, Ph.D., Department of Mechanical Engineering, University of Wisconsin-Madison, 1513 University Ave. Madison, WI 53706, Phone: 608-263-6692, Fax: 608-265-2316, easchmerr@wisc.edu.

Australian Football League, hamstring strains are the single most common injury with approximately six injuries per club per season, and 33% of those being recurrent injuries (24). The susceptibility of the hamstrings to injury during high speed running is likely linked to the biomechanical demands placed on the muscle, though debate continues as to whether injury is more likely during the stance or swing phase of a running gait cycle (22,32,37,40,53). Resolving this issue is relevant for designing the type of resistance training that may be most effective for preventing initial or recurrent injuries. Specifically, injury prevention programs would ideally incorporate aspects (e.g. lower extremity postures, muscle lengths, contraction type) that are most similar to the conditions associated with injury, such that the athlete can optimize the gains in functional strength (23) and minimize the risk of future injury.

Animal models have been used to establish relationships between musculotendon mechanics and injury risk. When stretching a maximally activated muscle, the degree of muscle injury is related to the magnitude of fiber strain and negative work done by the muscle (17,29,30). However when active stretch-shortening cycles are imposed on a musculotendon unit, the degree of strain taken up by the fibers can change with time, making the muscle potentially more susceptible to injury after repeated loading cycles (9). These insights are potentially relevant for understanding hamstring injury mechanisms. In particular, the biarticular hamstrings are known to undergo an active stretch-shortening contraction during the late swing phase of running gait (48,49), with the amount of negative work increasing significantly with running speed (10). Thus, the hamstrings may be susceptible to a late swing injury as a result of repetitive strides of high speed running (22,40). However, others have argued that the hamstrings are more likely to be injured during stance phase when the limb is subjected to external loading via foot-ground contact (32,37). Indeed, EMG activity indicates the hamstrings are active into stance phase (26,43,51). In addition, a recent study suggests that the hamstrings may also undergo a lengthening phase during late stance (53). However to date, there have been limited attempts to measure ground reactions during sprinting (27,33,36), and no prior studies that have used such data to analyze hamstring kinetics during stance.

The purpose of this study was to directly compare hamstring kinetics between stance and swing phases of a sprinting gait cycle. We hypothesized that peak loading and negative work would be greater during swing than stance, and that these measures would increase significantly with speed. The information obtained in this study provides a more complete understanding of hamstring demands during normal sprinting gait, which is important for scientifically assessing how specific exercises may be most effective in reducing injury rates.

Methods

Subjects

Twelve subjects (9 males, 3 females) volunteered to participate in this study (age: 24.5 ± 4.1 yrs, height: 176.1 ± 5.0 cm, mass: 70.2 ± 8.8 kg). The average maximum treadmill running speeds were 8.0 m/s and 7.1 m/s for males and females, respectively. All subjects had no prior surgical history in their lower extremity and had no lower extremity injury and/or pain in the three months prior to testing. The testing protocol was approved by the UW Institutional Review Board and all subjects provided informed consent in accordance with institutional policies.

Experimental protocol

Whole body kinematics were recorded using 42 reflective markers placed on the body segments of each subject; 23 of which were located on anatomical landmarks (Figure 1a). EMG activities were recorded from single differential surface electrodes (DE-2.1, DelSys, Inc, Boston, MA) placed on seven muscles of the right lower limb: biceps femoris (BF), medial hamstrings (semitendinosus (ST) and semimembranosus (SM)), vastus lateralis, rectus femoris and medial gastrocnemius. Each subject ran on an instrumented treadmill at a preferred speed to warm up, prior to sprinting at 80, 85, 90, 95, and 100% of his/her maximum speed, with a minimum of 5 strides (~5 s) collected at each speed. Two additional trials were collected to scale a biomechanical model to each subject: 1) a quiet standing position, to establish segment lengths, joint centers and joint coordinate systems, and 2) a hip circumduction movement (both the right and left sides), to determine functional hip joint centers (38).

Data acquisition

Three-dimensional kinematics were collected at 200 Hz using an 8-camera passive marker system (Motion Analysis Corporation, Santa Rosa, CA). Kinematic data were then low pass filtered using a bidirectional, 4^{th} order Butterworth filter with a cutoff frequency of 12 Hz. Three dimensional ground reaction forces and moments were also recorded at 2000 Hz using an instrumented treadmill (Bertec Corporation, Columbus, OH). These ground reactions were then low-pass filtered using a bidirectional 6^{th} order, low pass Butterworth filter with a cutoff frequency of 25 Hz. Foot contact and toe-off times were identified as the times when the vertical ground reaction force went above and then fell below 50 N.

EMG activities were interfaced to an amplifier unit (Bagnoli-16, DelSys, Boston, MA; CMRR > 84 dB at 60 Hz; input impedance > 100 MΩ) and recorded at 2000 Hz. The EMG signals were subsequently full-wave rectified and low pass filtered using a bidirectional, 6^{th} order Butterworth filter with a cutoff frequency of 20 Hz. Ensemble-average EMG activities were generated over the sprinting gait cycle by aligning foot strikes, normalizing to peak EMG activity and averaging activation patterns across multiple strides and subjects. For each muscle, the distribution of EMG activity over the gait cycle was quantified by computing the percentage of activity seen in three phases: stance phase (foot contact to toe-off), first half of swing phase (swing 1, toe-off to peak knee flexion) and second half of swing phase (swing 2, peak knee flexion to foot contact).

Musculoskeletal model

The body was modeled as a 14 segment, 31 degree of freedom (DOF) articulated linkage (Figure 1a). Anthropometric properties of body segments were scaled to each individual using the subject's height, mass, and segment lengths (12). The functional hip joint centers were used to scale the medio-lateral width of the pelvis. The hip joint was modeled as a ball and socket with three DOF. The knee joint was represented as a one DOF joint, in which the tibiofemoral translations and nonsagittal rotations were constrained functions of the knee flexion-extension angle (50). The ankle-subtalar complex was represented by two revolute joints aligned with anatomical axes (13). The lumbar spine was represented as a ball and socket joint at approximately the 3^{rd} lumbar vertebra (1). For each trial, joint angles were computed at each time step using a global optimization routine to minimize the weighted sum of squared differences between the measured and model marker positions (31).

Musculotendon actuators were represented by a series of line segments connecting the origin to the insertion with wrapping about joints and other structures accounted for with wrapping surfaces (4). The input to each musculotendon actuator was an idealized excitation level that varied between zero and one (full excitation). Muscle excitation-to-activation dynamics was

represented by a first order differential equation that had a faster time constant during activation (10 ms) than deactivation (30 ms). A Hill-type lumped parameter model (Figure 1c) of musculotendon contraction dynamics was used to relate activation to force, with muscle fibers assumed to be in series with an elastic tendon (39,54). Force produced by the musculotendon actuator was applied to the segment in which the tendon was attached.

Passive joint torques (eq. 1) were included to account for uniarticular, passive-elastic structures at the hip, knee and ankle; defined as a function of the joint angle (q) and angular velocity (u) with parameters (k_1, k_2, r_1, r_2, φ_1, φ_2, c) taken from literature (42).

$$T = k_1 e^{r_1 \cdot (q - \varphi_1)} + k_2 e^{r_2 \cdot (q - \varphi_2)} - c \cdot u \qquad \text{(eq. 1)}$$

The equations of motion of the musculoskeletal model were derived using SDFast (Parametric Technology Corporation, Waltham, MA) and SIMM Pipeline (Musculographics Inc., Chicago, IL).

Forward dynamic simulations

We generated muscle-actuated forward dynamic simulations of sprinting to characterize hamstring stretch, force and work. A total of 52 musculotendon actuators (26 actuators on each limb) were used to actuate two DOF on each limb (hip flexion-extension, knee flexion-extension). All other DOF were prescribed to follow the measured kinematic trajectories, thereby accounting for inter-segmental dynamics (55). Simulations were generated for a minimum of 5 strides at each speed for each subject (Figure 1d).

A computed muscle control (CMC) algorithm was used (10,44) to generate muscles excitations that drove the forward dynamic model to closely replicate experimental hip and knee kinematics. Muscle redundancy was resolved by using numerical optimization (20) to minimize the sum of the squared weighted normalized contractile element forces (eq. 2 and Figure 1b):

$$J = \sum_{i=1}^{num\ muscles} w_i \left(\frac{F_i^{CE}}{f_i(l_i^M) F_i^{\max}} \right)^2 \qquad \text{(Eq. 2)}$$

where the weighting factor, w_i is the volume of muscle i, F_i^{CE} is the contractile element force of muscle i, $f_i(l_i^{\mathrm{M}})$ is an active force-length scaling factor, and F_i^{max} is the maximum isometric force of muscle i. We included constraints in the optimization problem (no hamstring excitation from 20–40% gait cycle, and no rectus femoris excitation from 15–35% gait cycle) to ensure that hamstring and rectus femoris muscles were not excited when EMG data indicates they are not normally active (10).

Simulations were used to characterize the musculotendon stretch, force and power development of the biarticular hamstrings: BF, ST and SM. Musculotendon stretch was defined as the change in length of the musculotendon unit from an upright posture. Upright musculotendon lengths were computed by setting all joint angles to zero in the subject-specific scaled model. The musculotendon power generated (absorbed) was computed as the product of the force and musculotendon velocity. The negative and positive musculotendon work was computed by integrating the respective negative and positive portions of the power curves. The three biarticular hamstring musculotendon works were then added to obtain a measure of net negative and net positive hamstring musculotendon work.

Data Analysis

A two-way repeated measures analysis of variance was used to determine the effects of gait cycle phase and normalized speed (80, 85, 90, 95, and 100%) on the magnitude of peak force. A one-way repeated measures analysis of variance was then used to determine the effect of speed on net negative and net positive musculotendon work. Tukey's post hoc test was used to analyze significant main effects. The statistical analyses were completed using STATISTICA (version 6.0, StatSoft, Inc, Tulsa, OK, USA) with a significance level of 0.05 for all comparisons.

Results

The CMC algorithm generated simulations that closely tracked the experimental kinematics. Root mean squared error (RMS) for the hip and knee flexion/extension angles were 1.5 ± 0.5° for hip flexion-extension and 2.8 ± 0.8° for knee flexion-extension when the hamstrings were active. The pattern of predicted muscle excitations were generally similar to measured EMG activities (Figure 2). Mean hamstring excitations tended to be slightly less than measured EMG activities during the second half of swing phase, but were then greater than measured EMG magnitudes during stance (Figure 2, Table 1).

The hamstring musculotendons lengthened from approximately 50% to 90% of the gait cycle, with the negative work done only during swing phase (Figure 3). The hamstrings shortened and did positive work from 90% of the gait cycle throughout the subsequent stance phase. Net negative and positive musculotendon work both increased significantly ($p<0.001$) with speed (Figure 4); however, net negative hamstring work increased at a faster rate than positive work as speed increased (Figure 4).

Two distinct loading peaks were present for the hamstrings (Figure 3); one during late swing (between 85 and 95% of the gait cycle) and the second during early stance phase (between 0 and 15% of the gait cycle). A significant ($p<0.001$) speed by phase interaction was present for peak load of the BF and SM. Peak musculotendon force during swing increased significantly ($p<0.001$) with speed (Figure 3) for all 3 muscles (Table 2), while peak force during stance was independent of speed (Table 2; Figure 4). Peak swing phase force at the fastest speed exceeded peak stance phase force for the BF long head. At all speeds, the SM swing phase force exceeded the stance phase peak force. ST peak forces were not significantly different between swing and stance phase at the fastest speed (Table 2).

Discussion

In this study, we extended our prior analysis of hamstring kinetics during swing (10,45,46) to stance phase, thereby providing insights into when the hamstrings seem most susceptible to injury. The sprinting simulations predict that BF loading increases with speed during swing but not stance, and further that peak stretch and negative work demands occur exclusively during swing. These data lend further evidence to the belief that inertial loads put the lengthening hamstrings at risk for injury during high speed forward running (10,22,40). We do note that our analyses are limited to constant speed forward running; similar to the types of hamstring loading observed in a track sprinter. The hamstring loads that occur during sudden accelerations and turns could certainly factor into injury risk, and should be considered an important area of further study.

Prior studies of sprinting kinetics have been limited to joint level analyses (27,33,43). However, characterizing injury risk based solely on joint analysis is challenging due to the biarticular nature of the hamstrings. For example, peak hip and knee angles vary significantly with running speed (27,48), while peak hamstring stretch remains invariant as

sprinting speed increases (10). While increased hip flexion causes the hamstrings to be stretched this stretch can be offset by shortening from greater knee flexion at fast speeds (47). Similarly, it has been shown that hip and knee joint moments and powers increase with speed (27), but the associated biomechanical demands on the hamstrings are more difficult to determine.

Our results suggest that the hamstrings are substantially loaded during both the stance and swing phases of high speed treadmill running. However, we found that the hamstrings only undergo a lengthening contraction during late swing phase and thus negative muscle work is constrained to this phase. This result is similar to a number of prior kinematic studies (10,48,49,51), but contrasts with Yu, et al. (53), who reported that the hamstrings undergo a second lengthening period during the late stance phase of overground running. Conceptually, hamstring lengths are primarily a function of hip and knee flexion angles. For example, the hamstrings are lengthening during late swing when the hip is flexing and the knee is extending, as both of these motions contribute to hamstring stretch. However, the hip starts to extend prior to foot contact and continues to extend throughout stance (47); the knee flexes until mid-stance and then extends until toe-off. Therefore, if hamstring stretch is to occur during the second half of stance, the hamstring lengthening due to knee extension would have to exceed the hamstring shortening due to hip extension. Further because the hamstring moment arms at the hip are greater than at the knee (13,47), the knee extension velocity would have to exceed the hip extension velocity. However, sagittal hip and knee angular velocities during stance tend to be of comparable magnitude (27), making it unlikely that substantial hamstring stretch is occurring during stance.

Animal models of muscle injury show that active lengthening contractions are linked with injury (30), and that the degree of injury seems to be associated with the negative work done by a maximally activated muscle (8). In this study, we have shown that negative work performed by the hamstrings occurs exclusively during the swing phase, suggesting that the likelihood of a strain injury is greater during swing than stance. Further, hamstring loading was found to increase significantly with speed during swing but not stance, providing further support for injury susceptibility during the swing phase of high speed running. Repeated stretch shortening cycles have been shown to increase risk for injury in animal models (9), such that repeated strides of high speed running may contribute to the injury risk susceptibility.

There are a number of assumptions that are important when interpreting the model-based results in this study. First, we relied on literature-derived estimates for parameters such as tendon compliance, maximum isometric force, optimum fiber length, and musculoskeletal geometry (4,13). We have previously shown that tendon compliance can substantially influence estimates of muscle fiber stretch and work (46). For this reason, we limited our comparisons in this study to net musculotendon stretch and work, which are less dependent on specific musculotendon parameters (46). In addition, we note that the speed-dependent changes in peak loading and negative work were similar (Table 2) for all three biarticular hamstrings (which have different force capabilities, fiber lengths and geometries), which supports the idea that specific parameter assumptions did not pre-determine the observed results.

A numerical objective function, sum of weighted squared normalized forces (11), was used to resolve muscle redundancy. While predicted excitations were of comparable magnitude to normalized EMG activities during late swing (Table 1), the predicted BF excitation onsets were slightly delayed relative to EMG phasing (Figure 2). We used sensitivity analyses to determine how dependent the BF musculotendon force predictions are on excitation onset. We found that shifting the BF excitation onset time to 5% earlier in the gait cycle increased

the swing phase peak force by 4%, while having a small (<0.5%) effect on stance phase forces. These differences are less than the force discrepancies seen between stance and swing at the fastest running speed (Figure 3). Predicted hamstring excitation magnitudes during stance tended to be larger than measured EMG activities, while gastrocnemius excitations tended to be under-predicted in this phase (Figure 2, Table 1). This could be a result of not including active ankle actuation in the simulations, such that gastrocnemius excitation was not required to actively generate an ankle plantarflexion moment. Reduced gastrocnemius excitation also diminishes its contribution to the knee moment, and as a result hamstring excitation in early stance could have been over-estimated.

Measured ground reactions were directly applied to the feet, rather than dealing with the complexity of modeling the foot-floor interactions (2,18,19,34,35). We low-pass filtered the ground reactions at 25Hz, which is lower than is often done when analyzing running mechanics (15,25). This decision was based on a recent study by Bisseling and Hof (6), who suggested that using substantially different cutoff frequencies for kinematic and force data can introduce artificial peaks into computed joint kinetics (6). The 25Hz cutoff frequency adopted for this study was selected to mitigate this effect while retaining the high frequency information present in the ground reactions at contact. It is also important to recognize that one of our primary outcome measures (musculotendon work) is an integrated quantity, rather than an instantaneous quantity, and thus is less susceptible to choice of filter cutoff frequencies. However, we do note that the calculation of peak biomechanical loads during impact remains a challenging problem, and additional work on the appropriate selection of kinematic and kinetic filters (6) is warranted.

Defining the musculotendon demands during sprinting at the likely time of injury provides direction as to the type of resistance training that may prove most beneficial in preventing an initial or recurrent hamstring injury (23). For example, if injury occurs during the swing phase, which we suggest, then resistance training of the hamstrings may be most effective when performed with lower extremity postures that place the muscle in an elongated position (e.g., hip flexion with knee extension) (21). Further, lengthening (eccentric) contractions under inertial load would likely be an essential component of the prevention and rehabilitation strategy. This contraction-specificity with respect to hamstring injury prevention is supported in prior studies that demonstrated the successfulness of an eccentric-focused resistance training program (3,5,7). Finally, characterizing the load during the sprinting gait cycle enables the relative intensity of the resistance training to be more scientifically determined.

In conclusion, our data suggests that the hamstrings are at greater risk for injury during the late swing phase of high speed running when compared to stance phase. Late swing phase is when the biomechanical demands placed on the hamstrings seem most consistent with muscle injury mechanisms. Based on the results from this study, a rehabilitation program incorporating eccentric focused exercises is likely to have greater benefit over programs which focus on concentric loading of the hamstrings.

Acknowledgments

Funding for this research was provided by grants from the following: NIH (AR 56201, 1UL1RR025011), NFL Charities and an American Association of University Women Dissertation Fellowship that was award to E. Chumanov.

We acknowledge support from NIH Grants AR 56201, 1UL1RR025011, NFL Charities and an American Association of University Women Dissertation Fellowship to E. Chumanov. The results of this study do not constitute endorsement by the ACSM.

References

1. Anderson FC, Pandy MG. A dynamic optimization solution for vertical jumping in three dimensions. Computer Methods in Biomechanics and Biomedical Engineering 1999;2:201–231. [PubMed: 11264828]
2. Anderson FC, Pandy MG. Dynamic optimization of human walking. Journal of Biomechanical Engineering 2001;123:381–390. [PubMed: 11601721]
3. Arnason A, et al. Prevention of hamstring strains in elite soccer: an intervention study. Scand J Med Sci Sports 2008;18:40–8. [PubMed: 17355322]
4. Arnold AS, et al. Accuracy of muscle moment arms estimated from MRI-based musculoskeletal models of the lower extremity. Computer Aided Surgery 2000;5:108–19. [PubMed: 10862133]
5. Askling C, Karlsson J, Thorstensson A. Hamstring injury occurrence in elite soccer players after preseason strength training with eccentric overload. Scand J Med Sci Sports 2003;13:244–50. [PubMed: 12859607]
6. Bisseling RW, Hof AL. Handling of impact forces in inverse dynamics. Journal of Biomechanics 2006;39:2438–2444. [PubMed: 16209869]
7. Brooks JH, et al. Incidence, risk, and prevention of hamstring muscle injuries in professional rugby union. Am J Sports Med 2006;34:1297–306. [PubMed: 16493170]
8. Brooks SV, Zerba E, Faulkner JA. Injury to muscle fibres after single stretches of passive and maximally stimulated muscles in mice. Journal of Physiology 1995;488:459–69. [PubMed: 8568684]
9. Butterfield TA, Herzog W. Quantification of muscle fiber strain during in-vivo repetitive stretch-shortening cycles. Journal of Applied Physiology 2005;99:593–602. [PubMed: 15790684]
10. Chumanov ES, Heiderscheit BC, Thelen DG. The effect of speed and influence of individual muscles on hamstring mechanics during the swing phase of sprinting. Journal of Biomechanics 2007;40:3555–3562. [PubMed: 17659291]
11. Crowninshield RD, Brand RA. A physiologically based criterion of muscle force prediction in locomotion. Journal of Biomechanics 1981;14:793–801. [PubMed: 7334039]
12. de Leva P. Adjustments to Zatsiorsky-Seluyanov's segment inertia parameters. Journal of Biomechanics 1996;29:1223–30. [PubMed: 8872282]
13. Delp SL, et al. An interactive graphics-based model of the lower extremity to study orthopaedic surgical procedures. IEEE Transactions on Biomedical Engineering 1990;37:757–67. [PubMed: 2210784]
14. Feeley BT, et al. Epidemiology of National Football League Training Camp Injuries From 1998 to 2007. The American Journal of Sports Medicine 2008;36:1597–1603. [PubMed: 18443276]
15. Ferber R, Davis IM, Williams DSr. Gender differences in lower extremity mechanics during running. Clinical Biomechanics 2003;18:350–357. [PubMed: 12689785]
16. Gabbe BJ, Finch CF, Bennel KL, Wajswelner H. Risk factors for hamstring injuries in community level Australian football. British Journal of Sports Medicine 2005;39:106–110. [PubMed: 15665208]
17. Garrett WE Jr, et al. Biomechanical comparison of stimulated and nonstimulated skeletal muscle pulled to failure. Am J Sports Med 1987;15:448–54. [PubMed: 3674268]
18. Gerritsen K, van den Bogert AJ, Nigg BM. Direct dynamics simulation of the impact phase in heel-toe running. Journal of Biomechanics 1995;28:661–668. [PubMed: 7601865]
19. Gilchrist LA, Winter DA. A two-part, viscoelastic foot model for use in gait simulations. Journal of Biomechanics 1996;29:795–798. [PubMed: 9147977]
20. Happee R. Inverse dynamic optimization including muscular dynamics, a new simulation method applied to goal directed movements. Journal of Biomechanics 1994;27:953–60. [PubMed: 8063845]
21. Heiderscheit B, et al. Acute Hamstring Injuries: Recommendations for Diagnosis Rehabilitation and Injury Prevention. Journal of Orthopedic Sports Physical Therapy 2010;40:65–79.
22. Heiderscheit BC, et al. Identifying the time of occurrence of a hamstring strain injuring during treadmill running: a case study. Clinical Biomechanics 2005;20:1072–1078. [PubMed: 16137810]

23. Hortobágyi T, et al. Adaptive responses to muscle lengthening and shortening in humans. Journal of Applied Physiology 1996;80:765–72. [PubMed: 8964735]
24. Hoskins WT, Pollard H. Injuries in Australian Rules Football: A Review of the Literature. The Academy of Chiropractic Orthopedists 2003;11:49–56.
25. Hunter JP, Marshall RN, McNair PJ. Interaction of step length and step rate during sprint running. Med Sci Sports Exerc 2004;36:261–71. [PubMed: 14767249]
26. Jonhagen S, et al. Amplitude and timing of electromyographic activity during sprinting. Scandinavian Journal of Medicine and Science in Sports 1996;6:15–21. [PubMed: 8680937]
27. Kuitunen S, Komi PV, Kyrolainen H. Knee and ankle joint stiffness in sprint running. Medicine and Science in Sports and Exercise 2002;34:166–73. [PubMed: 11782663]
28. Kujala UM, Orava S, Jarvinen M. Hamstring injuries: current trends in treatment and prevention. Sports Medicine 1997;23:397–404. [PubMed: 9219322]
29. Lieber RL, Friden J. Muscle damage is not a function of muscle force but active muscle strain. Journal of Applied Physiology 1993;74:520–6. [PubMed: 8458765]
30. Lieber RL, Friden J. Mechanisms of muscle injury gleaned from animal models. American Journal of Physical Medicine and Rehabilitation 2002;81:S70–9. [PubMed: 12409812]
31. Lu TW, O'Connor JJ. Bone position estimation from skin marker coordinates using global optimisation with joint constraints. Journal of Biomechanics 1999;32:129–34. [PubMed: 10052917]
32. Mann R, Hagy J. Biomechanics of walking, running, and sprinting. American Journal of Sports Medicine 1980;8:345–350. [PubMed: 7416353]
33. Mann RV. A kinetic analysis of sprinting. Medicine and Science in Sports and Exercise 1981;13:325–328. [PubMed: 7321831]
34. Neptune RR, Kautz SA, Zajac FE. Contributions of the individual ankle plantar flexors to support, forward progression and swing initiation during walking. Journal of Biomechanics 2001;34:1387–1398. [PubMed: 11672713]
35. Neptune RR I, Wright C, van den Bogert AJ. A method for numerical simulation of single limb ground contact events: application to heel-toe running. Compative Methods of Biomechanical and Biomedical Engineering 2000;3:321–334.
36. Novacheck TF. Walking, running, and sprinting: a three-dimensional analysis of kinematics and kinetics. Instructional Course Lectures 1995;44:497–506. [PubMed: 7797888]
37. Orchard J, Best TM. The management of muscle strain injuries: an early return versus the risk of recurrence. Clinical Journal of Sport Medicine 2002;12:3–5. [PubMed: 11854581]
38. Piazza SJ, et al. Assessment of the functional method of hip joint center location subject to reduced range of hip motion. Journal of Biomechanics 2004;37:349–356. [PubMed: 14757454]
39. Sandercock TG, Heckman CJ. Force from cat soleus muscle during imposed locomotor-like movements: experimental data versus hill-type model predictions. Journal of Neurophysiology 1997;77:1538–1552. [PubMed: 9084618]
40. Schache A, et al. Biomechanical response to hamstring muscle strain injury. Gait and Posture 2009;29:332–338. [PubMed: 19038549]
41. Seward H, et al. Football injuries in Australia at the elite level. Medical Journal of Australia 1993;159:298–301. [PubMed: 8361423]
42. Silder A, et al. Identification of passive elastic joint moment-angle relationships in the lower extremity. Journal of Biomechanics 2007;40:2628–2635. [PubMed: 17359981]
43. Swanson S, Caldwell G. An integrated biomechanical analysis of high speed incline and level treadmill running. Medicine and Science in Sports and Exercise 2000;32:1146–1155. [PubMed: 10862544]
44. Thelen DG, Anderson FC. Using computed muscle control to generate forward dynamic simulations of human walking from experimental data. Journal of Biomechanics 2006;39:1107–1115. [PubMed: 16023125]
45. Thelen DG, Chumanov ES, Sherry M, Heiderscheit BC. Neuromusculoskeletal models provide insights into the mechanisms and rehabilitation of hamstring strains. Exercise Sport Science Reviews 2006;34:135–141.

46. Thelen DG, Chumanov Elizabeth S, Best Thomas M, Swanson Stephen C, Heiderscheit Bryan C. Simulation of biceps femoris musculotendon mechanics during the swing phase of sprinting. Medicine and Science in Sports and Exercise 2005;37:1931–1938. [PubMed: 16286864]
47. Thelen DG, Chumanov Elizabeth S, Hoerth Dina M, Best Thomas M, Swanson Stephen C, Li Li, Young Michael, Heiderscheit Bryan C. Hamstring muscle kinematics during treadmill sprinting. Med Sci Sports Exerc 2005;37:108–114. [PubMed: 15632676]
48. Thelen DG, Chumanov Elizabeth S, Hoerth Dina M, Best Thomas M, Swanson Stephen C, Li Li, Young Michael, Heiderscheit Bryan C. Hamstring muscle kinematics during treadmill sprinting. Medicine and Science in Sports and Exercise 2005;37:108–114. [PubMed: 15632676]
49. van Don, BJ. PhD Dissertation. The University of Iowa, Exercise Science; Iowa City: 1998. Hamstring injuries in sprinting.
50. Walker PS, Rovick JS, Robertson DD. The effects of knee brace hinge design and placement on joint mechanics. Journal of Biomechanics 1988;21:965–74. [PubMed: 3253283]
51. Wood G. Biomechanical limitations to sprint running. Medicine and Science in Sports and Exercise 1987;25:58–71.
52. Woods C, Hawkins RD, Maltby S, Hulse M, Thomas A, Hodson A. The football association medical research programme: an audit of injuries in professional football - analysis of hamstring injuries. British Journal of Sports Medicine 2004;38:36–41. [PubMed: 14751943]
53. Yu B, et al. Hamstring muscle kinematics and activation during overground sprinting. Journal of Biomechanics 2008;41:3121–3126. [PubMed: 18848700]
54. Zajac FE. Muscle and tendon: properties, models, scaling and application to biomechanics and motor control. Critical Reviews in Biomedical Engineering 1989;17:359–411. [PubMed: 2676342]
55. Zajac FE, Gordon ME. Determining muscle's force and action in multi-articular movement. Exercise and Sport Sciences Reviews 1989;17:187–230. [PubMed: 2676547]

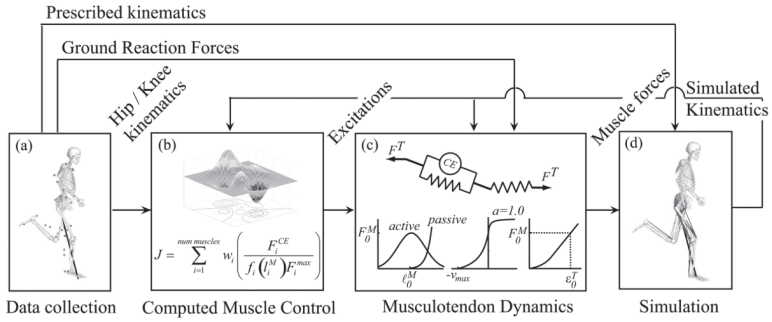

Figure 1.

A graphical depiction of how the simulations were generated. (a) Kinematic and kinetic data were first collected as each subject sprinted on a treadmill. (b) A computed muscle control algorithm (31) was used to generate the excitation patterns that drove the limb to closely track measured hip and knee kinematics. (c) Excitations were inputs into Hill-type models of musculotendon dynamics, which produce force that drive sagittal plane hip and knee motion. All other degrees of freedom were prescribed to follow measured trajectories, while ground reaction forces and moments were applied directly on the lower limbs. (d) Simulations were then generated, from which hamstring force, negative and positive work could then be determined.

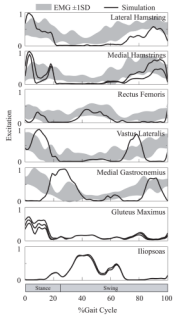

Figure 2.

At maximal sprinting speed (100%), the timing of simulated muscle excitations (solid lines, average over all subjects) and measured electromyographic (EMG) activities (shaded curves) are shown to be relatively consistent. EMG activities are the mean (± 1 s.d.) rectified, low-pass filtered activities over all subjects. In the model, the medial hamstrings (semitendinosus and semimembranosus) and iliopsoas (iliacus and psoas) are represented as two individual muscle line segments. Three line segments in the model were used to represent the broad attachments of gluteus maximus.

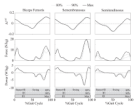

Figure 3.

The average musculotendon mechanics of the hamstring muscles over a simulated sprinting gait cycle for a representative subject. The length excursions ($\Delta \ell^{MT}$) of the hamstring musculotendons are relatively consistent across running speeds, with the lengthening phase constrained to swing phase. Peak swing phase musculotendon forces increased with speed for each of the hamstring muscles while stance phase peak forces remain invariant with speed. The hamstrings are stretching and do negative work (i.e. integral of negative power) on the system from 50 to 90% of the gait cycle, and then shorten and do positive work at the end of swing through stance phase.

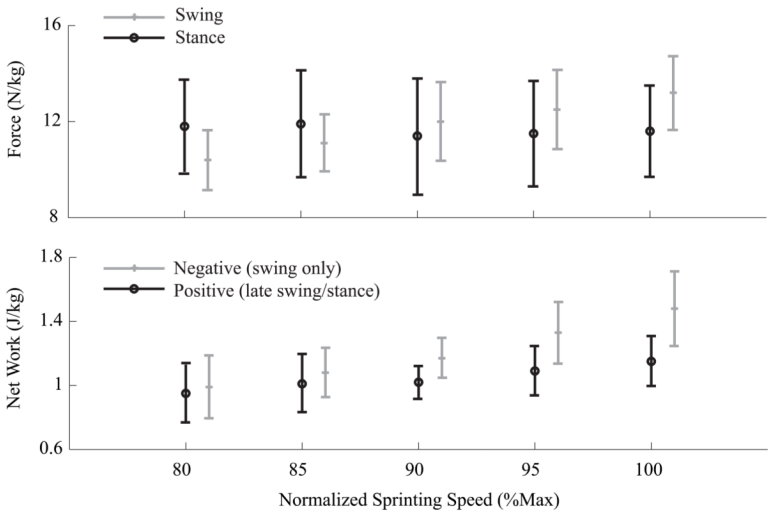

Figure 4.

Peak biceps femoris loading during swing phase significantly ($p<0.001$) increases with speed, and significantly ($p<0.003$) exceeds the loading incurred during stance at the fastest speed. Both net negative work and positive work increase as running speed increases, with net negative work increasing at a faster rate with speed than net positive work. The net work values shown are the sum of all three biarticular hamstring work (negative and positive).

Table 1

Comparison between the mean (sd) measured EMG activities and model-predicted excitations (EXC) over stance, and the first (swing 1) and second (swing 2) half of swing during the maximum speed (100%) sprinting gait cycle. EMG and excitations (EXC) magnitudes during each phase are expressed as a percentage of the mean activity over the full gait cycle. Stance is the phase between heel contact and toe off, swing 1 is from toe-off to peak knee flexion and swing 2 is from peak knee flexion to heel contact.

	Stance		Swing 1		Swing 2	
	EMG	**EXC**	**EMG**	**EXC**	**EMG**	**EXC**
Biceps Femoris	32 (12)	59 (11)	21 (10)	5 (9)	46 (11)	36 (6)
Medial Hamstrings	30 (14)	51 (11)	21 (11)	5 (8)	49 (11)	44 (7)
Rectus Femoris	30 (16)	34 (16)	44 (15)	53 (17)	26 (8)	13 (6)
Vastus Lateralis	31 (18)	64 (7)	20 (15)	8 (12)	50 (19)	29 (7)
Medial Gastrocnemius	42 (15)	35 (9)	18 (13)	34 (9)	40 (15)	31 (10)

Med Sci Sports Exerc. Author manuscript; available in PMC 2011 June 1.

Table 2

Mean (s.d.) kinematic and kinetic measures of the hamstring muscles across all subjects. Peak musculotendon stretch and the loading during stance phase were invariant across running speeds for the biceps femoris (BF), semimembranosus (SM) and semitendinosus (ST) muscle. However, swing phase peak force, and the positive and negative musculotendon work for all muscles increased significantly ($p<0.001$) with speed. Peak force during swing exceeded that of stance at the fastest speed for BF. The SM peak swing phase force exceeded stance phase force at all speeds, while stance and swing phase forces were comparable for the ST. $\Delta\ell^{MT}/\ell_o^{MT}$= peak musculotendon stretch normalized to its length in an upright posture, F^{Max} = peak musculotendon force, W^{MT}= work done by the musculotendon unit.

Measure	Speed (% max)	BF	SM	ST
Peak Stretch				
$\Delta\ell^{MT}/\ell_o^{MT}$	80	1.12 (0.02)	1.11 (0.02)	1.10 (0.02)
	85	1.12 (0.02)	1.11 (0.02)	1.10 (0.02)
	90	1.12 (0.02)	1.11 (0.02)	1.10 (0.02)
	95	1.13 (0.02)	1.11 (0.02)	1.11 (0.02)
	100	1.13 (0.02)	1.11 (0.03)	1.10 (0.03)
Peak Stance Phase Force				
${}^{2}F^{Max}(N/kg)$	80	11.8 (1.9)	12.5 (3.2)	5.5 (2.1)
	85	11.9 (2.2)	12.2 (2.7)	5.7 (2.1)
	90	11.4 (2.4)	11.9 (2.4)	6.0 (2.1)
	95	11.5 (2.2)	11.9 (2.3)	5.8 (1.9)
	100	11.6 (1.9)	12.1 (2.4)	6.2 (2.2)
Peak Swing Phase Force				
${}^{1,2}F^{Max}(N/kg)$	80	10.4 (1.2)	18.6 (2.2)	4.8 (1.3)
	85	11.1 (1.2)	19.9 (2.8)	5.2 (1.6)
	90	12.0 (1.6)	21.8 (3.6)	5.3 (1.5)
	95	12.5 (1.6)	23.0 (3.8)	5.3 (1.4)
	100	13.2 (1.5)	23.9 (3.5)	5.9 (1.9)
Positive Work				
${}^{1}W^{MT}(J/kg)$	80	0.36 (0.06)	0.42 (0.08)	0.18 (0.05)
	85	0.37 (0.06)	0.43 (0.08)	0.21 (0.05)
	90	0.38 (0.05)	0.43 (0.05)	0.22 (0.03)
	95	0.40 (0.06)	0.45 (0.07)	0.24 (0.05)
	100	0.43 (0.06)	0.47 (0.08)	0.26 (0.04)
Negative Work				
${}^{1}W^{MT}(J/kg)$	80	0.31 (0.09)	0.48 (0.09)	0.19 (0.04)
	85	0.33 (0.07)	0.51 (0.05)	0.23 (0.06)
	90	0.36 (0.05)	0.56 (0.05)	0.25 (0.05)
	95	0.41 (0.07)	0.63 (0.10)	0.28 (0.05)
	100	0.46 (0.09)	0.69 (0.10)	0.35 (0.06)

[1] Significant speed effect

[2] Significant speed by gait cycle phase interaction for BF and SM